ADVANCED FUNCTIONAL MATERIALS
www.afm-journal.de

Inwards Interweaving of Polymeric Layers within Hydrogels: Assembly of Spherical Multi-Shells with Discrete Porosity Differences

*Houwen Matthew Pan, Sebastian Beyer, Qingdi Zhu, and Dieter Trau**

The unique inwards interweaving morphology of polyamines and polyacids within agarose hydrogels that leads to the formation of striated shells with different porosities within the spherical scaffold is reported. Microcompartments with sophisticated structures are commonly used in drug delivery, tissue engineering, and other biomedical applications. However, a method capable of producing well-defined, multiporous shells within a single compartment is still lacking. By the alternating deposition of polyallylamine (PA) and polystyrenesulfonic acid (PSS) in 1-butanol, at equal mass ratios, multiple levels of porosity are generated within an agarose microsphere. Each level of porosity is represented by a well-defined, concentric shell of interweaving PA and PSS layers. The number, thickness, and porosity of the striated shells can be easily controlled by varying the number of PA/PSS bilayers and the polymer concentration, respectively. The feasibility of utilizing this morphology for the assembly of a multi-shell porous spherical scaffold is validated by trapping different molecular weight dextrans within different regions of porosity. The unique interaction of polyacids and polyamines in hydrogels represents a facile and inexpensive approach to the development of intricate scaffold architectures.

1. Introduction

Microcompartments with complex 3D structures are attractive as materials in chemical sensors,[1,2] drug delivery[3,4] and tissue engineering.[5,6] Polymeric hydrogel capsules, in particular, are ideal for the creation of sophisticated microcompartments due to their facile tunability, good biocompatibility and highly aqueous three-dimensional network.[7–9] Furthermore, the porosity of hydrogels allows for efficient mass transport and free diffusion of sensitive molecules.

H. M. Pan, Dr. D, Trau
Department of Bioengineering
National University of Singapore
7 Engineering Drive 1, 117574, Singapore
E-mail: bietrau@nus.edu.sg
Dr. S. Beyer
Singapore-MIT Alliance for Research and Technology (SMART) Centre
BioSystems and Micromechanics (BioSym) Interdisciplinary Research Group
Singapore, 1 CREATE Way, #04-13/14 Enterprise Wing, Singapore 138602
Dr. Q. Zhu, Dr. Trau
Department of Chemical & Biomolecular Engineering
National University of Singapore
4 Engineering Drive 4, 117576, Singapore

DOI: 10.1002/adfm.201300733

There had been numerous reports on multicompartment and multishell assemblies. In recent years, utilizing $CaCO_3$ particles as templates, four different multicompartmentalization strategies were developed: concentric, pericentric, innercentric and anisotropic.[10–12] In particular, enzyme-catalyzed reactions were demonstrated using multicompartmentalized, porous $CaCO_3$ particles carrying substrate and enzyme in separate subcompartments.[13,14] With agarose or alginate hydrogel as templates, the unique organic-phase phenomenon, inwards buildup of concentric polymeric layers was demonstrated to produce discrete multishells within a compartment.[15] Despite the array of multicompartment assemblies available, a method capable of producing well-defined, multiporous shells within a single compartment is still lacking. This would allow to separate biomolecules based on molecular weight and greatly complement current compartmentalization strategies.

Therefore, we present here the unique inwards interweaving morphology of polyamines and polyacids within agarose hydrogels to produce spherical multi-shells with discrete porosity differences. This is achieved by the alternating deposition of polyallylamine (PA) and polystyrenesulfonic acid (PSS) in 1-butanol, at equal mass ratios (**Figure 1**). This creates multiple levels of porosity, each comprising of different number of interweaving layers. The number and thickness of different levels of porosity can be easily tuned by varying the number of PA/PSS bilayers deposited and the polymer concentration respectively. We also demonstrate the feasibility of utilizing this morphology for the assembly of a multi-shell porous structure by the entrapment of different molecular weight dextrans within different tiers of porosity.

2. Results and Discussion

2.1. Comparison Between Inwards Interweaving Self-Assembly and the Inwards Buildup Self-Assembly

The inwards interweaving of polymeric layers is a unique interaction that occurs only in an organic phase, between

© 2013 WILEY-VCH Verlag GmbH & Co. KGaA, Weinheim

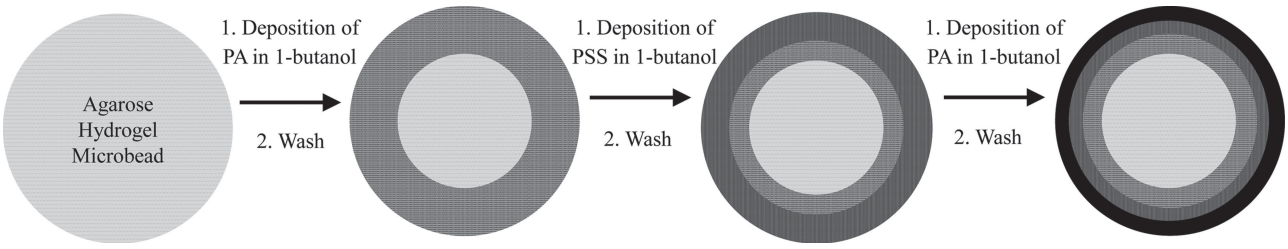

Figure 1. Process scheme for the preparation of inwards interweaving of polymeric layers within an agarose hydrogel microbead. Interweaving layers of polymer are assembled within the agarose hydrogel matrix by alternating deposition of polyallylamine (PA) and polystyrene sulfonic acid (PSS) in an organic phase (1-butanol).

polyamines (PA) and polyacids (PSS) within a porous hydrogel (agarose) matrix. In order to elucidate the driving force behind this polymer interaction, we will need to first examine the previously reported inwards buildup self-assembly process.[15]

For inwards buildup, successive polymeric layers are always formed after diffusing through earlier formed layers, assembling discrete layers in an inward fashion (**Figure 2**D–F). This inwards diffusing behaviour of polymer is observed only in organic solvent-based processes. For aqueous solvent-based methods, such as the conventional layer-by-layer (LbL) polyelectrolyte self-assembly, polyelectrolytes are highly ionic and strong electrostatic intra- and interchain repulsions exist. As a result, only partial interdiffusion of polymer occurs and micrometer-thick layers cannot be formed from single polymer incubations.[16,17] In contrast, polymer molecules that are completely dissolved in alcohol (1-butanol) are only very weakly ionic, due to auto-dissociation, and ionic repulsions are significantly reduced.[18] By applying this organic-phase polymer assembly process to the macroporous agarose gel network,[19] a complete inwards diffusion of polymer can be achieved. Therefore, the inwards buildup self-assembly process is not self-limited and micrometer-thick layers can be formed.

There are two possible interactions that could be responsible for the PA-agarose linkage. One of them could be the electrostatic interaction between polyallylamine and charged moieties within agarose to produce an ionic bond.[20] Sulfate is the main ionic group in agarose[21,22] and is present in minute quantities (<0.3%) in the agarose used in our experiments. Alternatively, inwards buildup could also be driven by hydrogen bonding. We hypothesize that the groups responsible for such a PA-agarose linkage are the outward-pointing O atoms and–OH groups of agarose which are free to engage in hydrogen bonding with PA molecules.[19] The amine functional groups of PA could serve as both hydrogen bond donors and acceptors because of the electronegative N atom and electropositive H atoms.

The same inwards buildup phenomenon has also been observed for alginate gels.[15] Even for an ionic polysaccharide like alginate, hydrogen bonds are reported to have an important role in stabilizing gel formation.[23] Alginate gels also have a highly porous structure.[24] Therefore, we believe that the above-mentioned chemical and physical properties are crucial towards establishing an inwards buildup mechanism.

Interestingly, the alternating deposition of PA and PSS, instead of a single PA deposition, is sufficient to yield a drastically different phenomenon. Instead of growing inwards, successive PSS or PA polymeric layers are now observed to be interweaving within the peripheral matrices of the macroporous hydrogel (Figure 2A–C). In Figure 2B, a yellow concentric outer ring is observed due to the overlapping of PA-TRITC and PSS-FITC layers. Similarly, an orange concentric outer ring is observed on Figure 2C because of the overlapping of PA-TRITC, PSS-FITC and the second PA-TRITC layer. Furthermore, the thickness of successive polymeric layers decreases with each deposition of PA or PSS (**Figure 3**). The same phenomenon was also observed for different sizes of agarose microbeads (Figure S1,

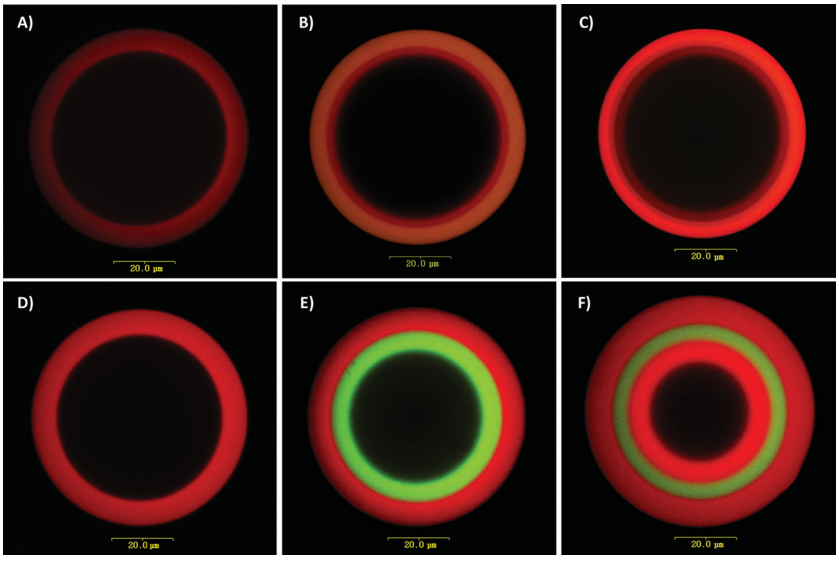

Figure 2. Confocal fluorescence images demonstrating the different morphology of striated shells obtained by A–C) the inwards interweaving mechanism in comparison to the previously reported D–F) inwards buildup mechanism. Agarose hydrogel microbeads are assembled with different number and type of polymer layers in the organic phase: A,D) one layer PA-TRITC, B) two layers (PA-TRITC/PSS-FITC), C) three layers (PA-TRITC/PSS-FITC/PA-TRITC), E) two layers (PA-TRITC/PA-FITC), and F) three layers (PA-TRITC/PA-FITC/PA-TRITC). A polymer concentration of 0.1 mg mL^{-1} and incubation time of 30 min were used for all experiments.

© 2013 WILEY-VCH Verlag GmbH & Co. KGaA, Weinheim

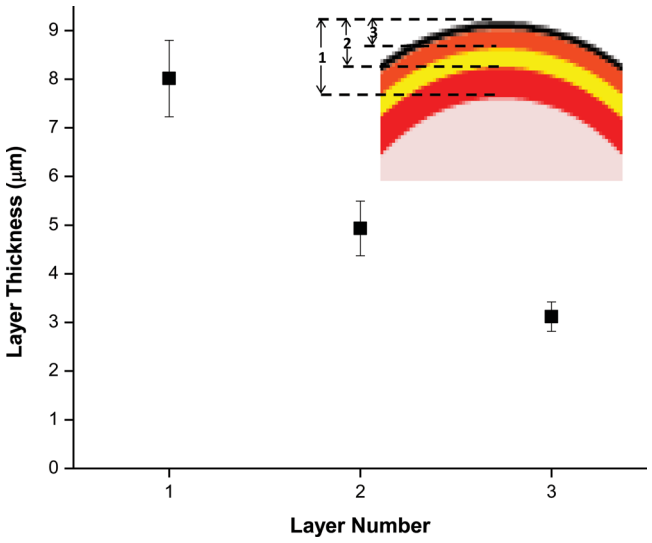

Figure 3. Layer thickness of concentric layers as a function of layer number for agarose microbeads assembled with the layers PA-TRITC/PSS-FITC/PA-TRITC. A polymer concentration of 0.1 mg mL^{-1} and incubation time of 30 min were used for all experiments. Measurements were made from capsules ranging 30 to 60 μm in diameter, dispersed in the organic phase. Inset: Definition of layer number.

Supporting Information). The concentration of polymer, agarose microbeads and incubation time is kept constant for each deposition.

The interweaving of polymers is in direct contrast to that observed by Zhang et al. in the fusion of polyelectrolyte microcapsules.[25] In their work, polyelectrolyte molecules entangle due to the loss of charges and hydrophobic interactions and hence do not mix with polyelectrolytes from a separate capsule. This observation provides some indication that the predominant interaction driving the interweaving of PSS and PA is non-hydrophobic. We propose that an ionic PA-PSS linkage is formed during the interweaving process. Upon incubation with PSS, protonation of the amine groups on PA by the sulfonic acid groups on PSS will induce a positive charge. The negatively charged PSS (autoprotolysis) then interacts electrostatically with PA, forming numerous stable ionic bonds. A similar mechanism is described by Beyer et al. for the interaction of polymers in an organic phase.[18,26] This leads to the arrest of inwards buildup and gives rise to an inwards interweaving of polymeric layers within a hydrogel matrix.

Despite a fixed incubation time and initial mass concentration of polymer, a decrease in thickness of successive layers is observed as layer number increases. This can be explained by the decrease in porosity of the agarose gel. As the number of polymer deposition increases, polymer molecules will start clogging up the pores of the agarose gel due to the increase in density of interweaving polymers. This will reduce the porosity of the hydrogel structure and the diffusion rate of polymers will also decrease. Eventually, this leads to a decrease in thickness of successive layers for the same incubation time and polymer mass concentration. For inwards buildup, it was reported that less polymer enters the hydrogel matrix as more polymers get deposited. This is likely due to the same decrease in porosity.

For the inwards interweaving self-assembly, polymeric layers interweave within the porous agarose matrix. This is in direct contrast with the diffusion of polymers through previously formed layers for the inwards buildup mechanism. As a result, no increase in polymer wall thickness will be observed. Instead, the density of the outermost polymer layer increases with each deposition.

2.2. Tuning of Thickness of Interweaving Layers

We studied the change in thickness of the PSS layer for agarose microbeads deposited with different mass ratios of PA:PSS-FITC. This was carried out by using an increasing concentration of PSS-FITC while maintaining a constant PA concentration of 0.1 mg mL^{-1}. A PA concentration of 0.1 mg mL^{-1} was used because for lower polymer concentrations (≤0.1 mg mL^{-1}), the thickness of the polymer layer is relatively constant across different bead sizes (Figure S2, Supporting Information). As expected, the thickness of the fluorescent layer increased only initially, and remained constant for all higher mass ratios (**Figure 4**A). Additionally, the maximum thickness of the fluorescent layer, about 8 μm, is similar to that of the first PA layer deposited, 8.0 μm ± 0.8 μm (Figure 3). This could also be observed from confocal fluorescence images (**Figure 5**). In Figure 4B, the average fluorescence intensity of the fluorescent layer is much higher (more than three times) than that of the agarose interior. This corresponds to a much higher PSS polymer density in the fluorescent layer than in the agarose interior.

The results indicate that the thickness of the much denser fluorescent layer is limited by the thickness of the PA layer. The higher polymer density is likely due to the formation of ionic complexes by PSS and PA. Once the PA layer has been completely complexed, further increase in mass concentration of PSS will lead to inwards buildup, forming PSS-agarose complexes in the agarose interior. The lower PSS polymer density in the agarose interior could be due to the repulsion experienced by negatively charged PSS and agarose molecules, resulting in a much lower packing density.

Next, we investigated the change in thickness of the PA layer for agarose microbeads incubated with different mass ratios of PA:PSS:PA-FITC. A fixed PA and PSS concentration of 0.1 mg mL^{-1} was used with increasing concentrations of PA-FITC. Comparable to our results with PSS, the thickness of the outer fluorescent layer increased only initially, and remained constant for all higher mass ratios (**Figure 6**A). Moreover, the maximum thickness of the outer fluorescent PA layer, about 4.5 μm, is similar to that of the second PSS layer, 4.9 μm ± 0.6 μm (Figure 3). The same observation could be made from comparing the confocal fluorescence images shown in **Figure 7**. However, for mass ratios of 1:1:2.5 and above, a dense inner fluorescent layer was formed, separated from the outer fluorescent layer by a non-fluorescent layer (Figure 7B). An occurrence not observed for PSS depositions. Furthermore, the average fluorescence intensity of the outer fluorescent layer is higher than

© 2013 WILEY-VCH Verlag GmbH & Co. KGaA, Weinheim

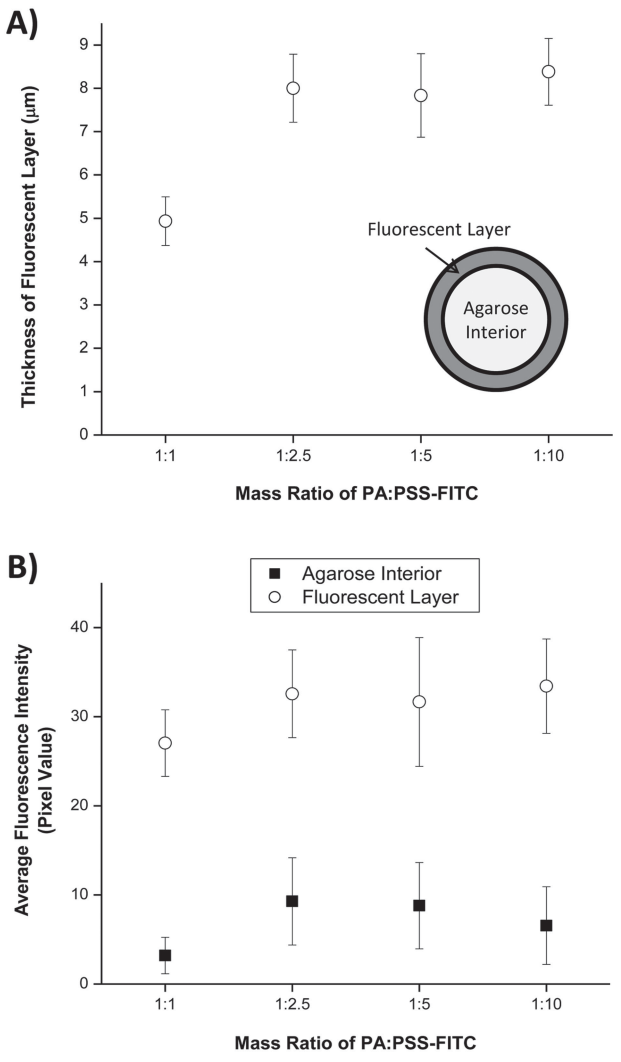

Figure 4. Graphs of A) thickness of fluorescent layer vs. mass ratio of PA:PSS-FITC and B) average fluorescence intensity of fluorescent layer and agarose interior vs. mass ratio of PA:PSS-FITC. Agarose microbeads were assembled with two layers (PA/PSS-FITC). Only the concentration of PSS-FITC was varied. A fixed PA concentration of 0.1 mg mL^{-1} was used. Measurements were made from capsules ranging 30 to 60 μm in diameter, dispersed in the organic phase. Inset: Definition of agarose-polymer components.

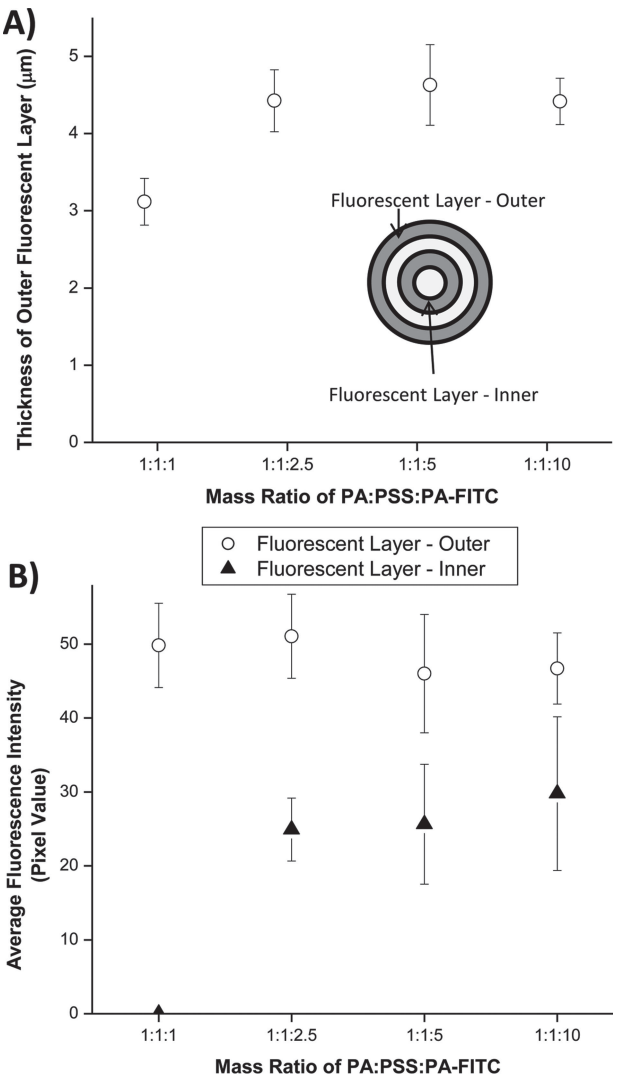

Figure 6. Graphs of A) thickness of outer fluorescent layer vs. mass ratio of PA:PSS:PA-FITC and B) average fluorescence intensity of outer and inner fluorescent layers as a function of mass ratio of PA:PSS:PA-FITC. Agarose microbeads were assembled with three layers (PA/PSS/PA-FITC). Only the concentration of PA-FITC was varied. A fixed concentration of 0.1 mg mL^{-1} was used for PA and PSS. Measurements were made from capsules ranging 30 to 60 μm in diameter, dispersed in the organic phase. Inset: Definition of agarose-polymer components.

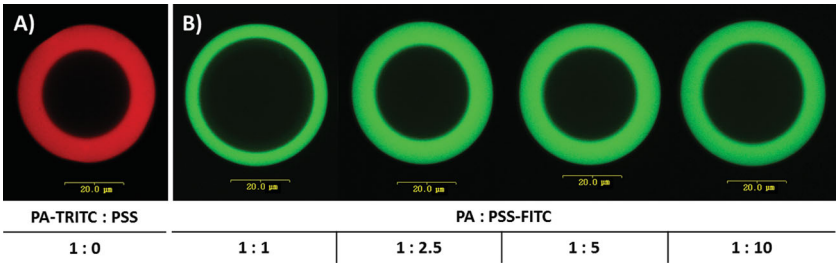

Figure 5. Confocal fluorescence images of agarose beads assembled with A) one layer PA-TRITC and B) two layers (PA/PSS-FITC). Different mass ratios of PA:PSS-FITC were assembled by using increasing concentrations of PSS-FITC (0.1 to 1 mg mL^{-1}) for a fixed concentration of PA (0.1 mg mL^{-1}). Scale bars represent 20 μm.

that of the inner fluorescent layer, suggesting a higher polymer density (Figure 6B).

Similarly, the results indicate that the thickness of the denser outer fluorescent layer is limited by the thickness of the PSS layer. However, as the mass concentration of PA increases, the PSS layer will be completely complexed and excess PA molecules would diffuse inwards, pass the non-fluorescent PA layer to form PA-agarose complexes in the agarose interior. The higher PA polymer density observed in the outer fluorescent layer could be due to the stronger

© 2013 WILEY-VCH Verlag GmbH & Co. KGaA, Weinheim

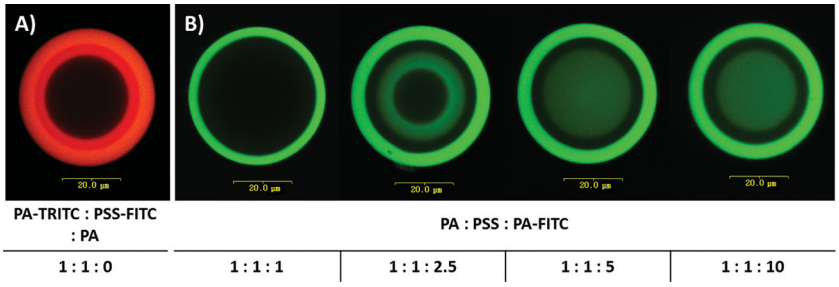

Figure 7. Confocal fluorescence images of agarose beads assembled with A) two layers (PA-TRITC/PSS-FITC) and B) three layers (PA/PSS/PA-FITC). Different mass ratios of PA:PSS:PA-FITC were assembled by using increasing concentrations of PA-FITC FITC (0.1 to 1 mg mL^{-1}) for a fixed concentration of PA and PSS (0.1 mg mL^{-1}). Scale bars represent 20 μm.

electrostatic interactions between protonated PA and deprotonated PSS molecules, leading to a much higher packing density. In comparison, the interaction between agarose and PA molecules is much weaker.

2.3. Assembly of Spherical Multi-Shells with Discrete Porosity Differences

The inwards interweaving of polymeric layers represents a process that generates unique morphologies that could be applied for the assembly of striated shells with discrete porosity differences. Based on our results, we have established that by alternating the deposition of PA and PSS, at equivalent mass ratios, well-defined concentric regions of different number of interweaving layers can be assembled. This is demonstrated in **Figure 8**, where six polymer layers $(PA\text{-}FITC/PSS)_3$ have been interweaved into the porous matrix of an agarose microsphere. Each concentric region corresponds to a distinct porosity, controlled by the density of the interweaving layers. By increasing the number of PA/PSS depositions, we are able to generate multiple levels of porosity within a single hydrogel microsphere.

In order to validate the feasibility of our unique morphology for the assembly of a multi-shell porous spherical scaffold, we encapsulated different molecular weight dextrans (M_w 3–5 kDa, 65–85 kDa and 2000 kDa) and transferred the microspheres from 1-butanol into an aqueous buffer. The confocal results show that different molecular weight dextrans are trapped in different porosity regions within the microsphere (**Figure 9**B, D, F). This is caused by the out-diffusion of dextran molecules, driven by the concentration gradient between the capsule interior and the exterior aqueous environment. The entrapment of dextran molecules within polyelectrolyte membranes has also been reported by other groups.[27,28] The fluorescence intensity plot profiles revealed that 2000 kDa dextran molecules are mainly trapped within the core of the porous agarose matrix (Figure 9A). 65–85 kDa dextran molecules are mainly trapped within the inner polymer layer, formed from two interweaved polymer layers (PA/PSS) (Figure 9C). Dextran molecules in the size of 3–5 kDa were observed to have partially diffused out of the capsule and the remaining molecules are spread between the outer $(PA/PSS)_2$ and inner (PA/PSS) polymer layers (Figure 9E). The diffusion patterns of the different molecular weight dextrans indicate a clear relation between the porosity of the interweaving polymer layers and the size of the molecule. The larger the size of the molecule, the lower the porosity of the structure required to trap them.

3. Conclusions

We have demonstrated that polyallylamine (PA) and polystyrenesulfonic acid (PSS) interweave in an inwards fashion within agarose hydrogels. Through alternating depositions of PA/PSS bilayers at equal mass ratios, with

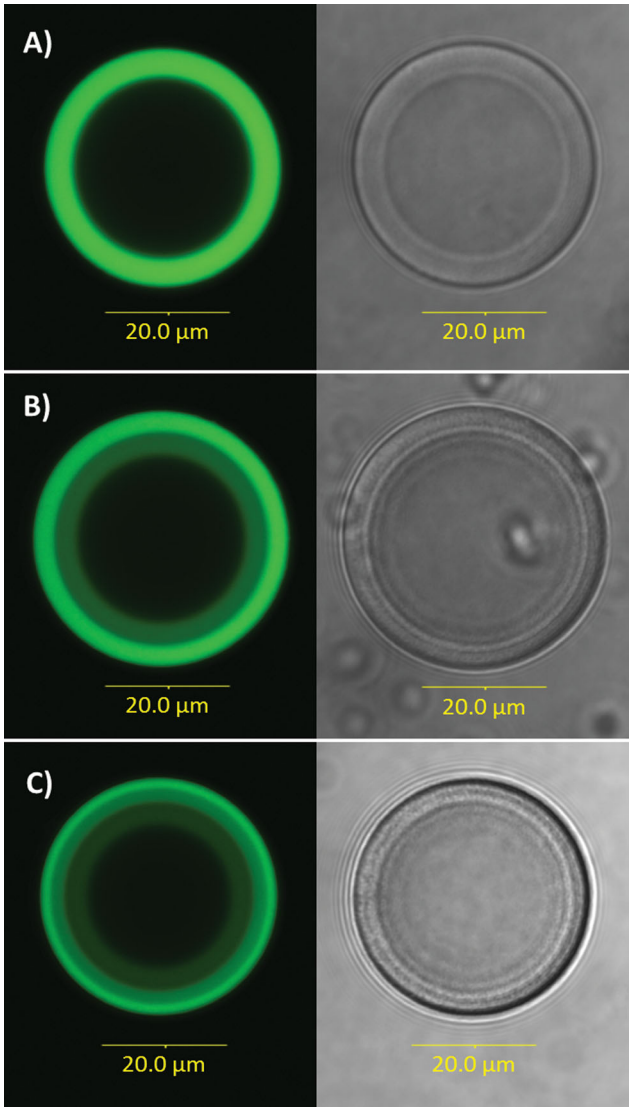

Figure 8. Confocal fluorescence and corresponding differential interference contrast images of agarose beads assembled with A) two layer (PA-FITC/PSS), B) four layers $(PA\text{-}FITC/PSS)_2$, and C) six layers $(PA\text{-}FITC/PSS)_3$. A fixed concentration of 0.1 mg mL^{-1} was used. Gain settings for each image are separately optimized for easier visualization.

© 2013 WILEY-VCH Verlag GmbH & Co. KGaA, Weinheim

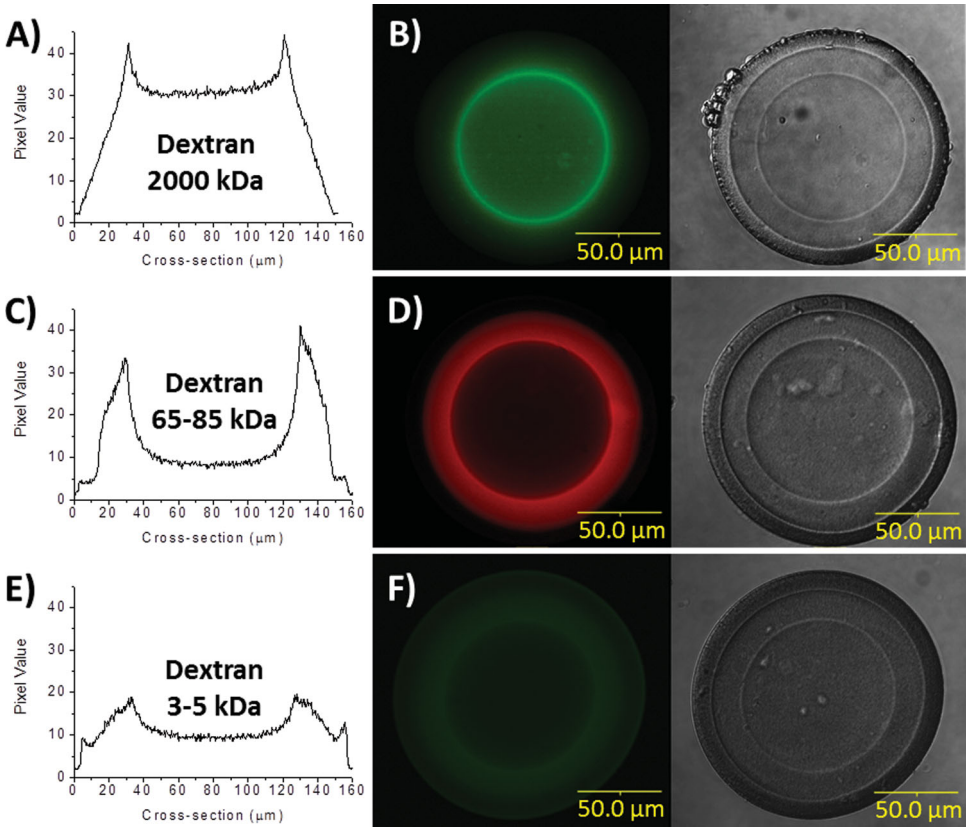

Figure 9. A,C,E) Fluorescence intensity plot profiles and B,D,F) confocal fluorescence and corresponding differential interference contrast images of different molecular weight dextrans trapped in different porous regions within the agarose microcapsule. Agarose capsules were assembled with four layers $(PA/PSS)_2$ and encapsulated A,B) 2000 kDa dextran, C,D) 65–85 kDa dextran and E,F) 3–5 kDa dextran. A fixed polymer concentration of 0.5 mg mL^{-1} was used.

all other parameters kept constant, multiple tiers of porosity can be fabricated, each comprising of different number of interweaving PA and PSS layers. The higher the density of interweaving layers, the lower the porosity. We also showed that the thickness and number of different tiers of porosity can be easily tuned by varying the polymer concentration and number of PA/PSS depositions respectively. Lastly, the diffusion patterns of dextran of different size fractions indicate that the larger the size of the dextran molecule, the lower the porosity of the structure required to trap it. This result successfully demonstrates the assembly of a multi-shell porous spherical scaffold.

In summary, the interweaving of polyacids and polyamines in hydrogels represents a facile approach to create multi-shells with discrete porosity differences. Work is currently under way with different polyamine and polyacid (e.g., polyethyleneimine and polyacrylic acid) alternatives to generate a wider range of scaffold porosity and create even more interesting geometries. Biodegradable polymers (e.g., poly-L-lysine and poly-L-glutamic acid) can also be incorporated as alternate layers to produce structures with free intermembrane spaces. With the wide range of polyamines and polyacids available (highly branched, biodegradable, biostable, etc.), we could potentially create a limitless range of complex geometries. This would complement current multicompartmentalization strategies and allow even greater control over the release and separation of biomolecules.

4. Experimental Section

Materials: Dextran-FITC (M_w 3000–5000 g mol^{-1} and 2 000 000 g mol^{-1}), Dextran-TRITC (Mw 65 000–85 000 g mol^{-1}), fluorescein isothiocyanate (FITC), tetramethylrhodamine isothiocyanate (TRITC), 1-butanol anhydrous 99.8%, low gelling point agarose and mineral oil were purchased from Sigma. Span 80 was purchased from Fluka. Poly(allylamine) 20% solution in water (M_w 65 000 g mol^{-1}) and ADOGEN 464 were purchased from Aldrich. Poly(styrenesulfonic acid) 30% solution in water (M_w 70 000 g mol^{-1}) was purchased from Polysciences. Absolute ethanol was purchased from Fisher Scientific. PBS buffer was purchased from 1st BASE.

Preparation of Poly(allylamine) and Poly(styrenesulfonic acid) in 1-Butanol: Poly(allylamine) (PA) in 1-butanol was prepared by completely drying the purchased aqueous PA solution at 55 °C, followed by fully saturating 1-butanol with the dried PA. 1 mL of the saturated 1-butanol was dried and weighed to determine the actual PA concentration. The solution was then diluted with 1-butanol to prepare a 1 mg mL^{-1} PA solution. This was used as stock solution. Fluorescence labeled PA was prepared by dissolving and reacting FITC or TRITC with PA in 1-butanol at a ratio of 1:100 (fluorophore:PA monomer). Lower concentrations of PA/PA-FITC or PA/PA-TRITC were prepared by diluting the 1 mg mL^{-1} PA stock solutions. Poly(styrenesulfonic acid) (PSS) in 1-butanol was

© 2013 WILEY-VCH Verlag GmbH & Co. KGaA, Weinheim

prepared by completely drying the PSS solution at 55 °C and re-dissolving in 1-butanol to produce a concentration of 1 mg mL^{-1}. This was used as the stock solution.

Preparation of Agarose Microbeads by Mechanical Stirring: A 4% w/v low-melting agarose in deionized H_2O was prepared and kept molten at a temperature of 40 °C. All other reagents and equipment used were pre-warmed and kept at a temperature of 40 °C. The molten agarose was then mixed with the desired biomolecule solution (Dextran) at a 1:1 volume ratio to prepare a mixture with a final concentration of 2% w/v agarose containing the desired concentration of biomolecules. 200 µL of biomolecule agarose mixture was added to 4800 µL of mineral oil containing 0.1% Span 80 and stirred vigorously for 10 min to form water-in-oil emulsion droplets. The droplets were then cooled in an ice water bath under stirring for another 10 min to allow solidification of the molten agarose droplets into agarose microbeads. The solidified agarose microbeads were further stabilized by placing at 4 °C for 10 min.

Transfer of Agarose Microbeads into the Organic Phase: An equal volume of ethanol containing 0.5% ADOGEN 464 was added to the agarose-in-oil suspension and mixed vigorously, followed by centrifugation. The mineral oil and ethanol supernatant was then discarded and the pellet containing the agarose microbeads was washed twice with 1-butanol containing 0.5% ADOGEN 464. ADOGEN 464 is added to prevent dehydration and aggregation of agarose beads in the organic phase.

Fabrication of Polymeric Hydrogel Capsules via Inwards Buildup Self-Assembly: 200 µL of agarose microbeads suspended in organic phase were incubated with 1 mL of the desired concentration of PA or PSS in 1-butanol containing 0.5% ADOGEN 464 for 30 min under gentle vortexing, followed by removal of excess polymer by two washing and redispersion cycles using the same organic medium. This forms the first concentric polymeric layer. Incubation with the same polymer solution was repeated until the desired number of concentric polymeric layers was achieved.

Fabrication of Polymeric Hydrogel Capsules via Inwards Interweaving Self-Assembly: 200 µL of agarose microbeads suspended in organic phase were incubated with 1 mL of the desired concentration of PA in 1-butanol containing 0.5% ADOGEN 464 for 30 min under gentle vortexing, followed by removal of excess polymer by two centrifugation and redispersion cycles with 1-butanol containing 0.5% ADOGEN 464. The second layer was deposited by incubation with 1 mL PSS solution at the desired concentration in the same organic medium. After the adsorption process, excess polymer was removed by two centrifugation and redispersion cycles with the organic medium. Alternating deposition of PA and PSS onto the agarose microbeads was performed until the desired number of layers was achieved.

Polymeric Layer Thickness and Density Studies: Agarose microbeads pre-assembled with 0.1 mg mL^{-1} PA or PA/PSS were incubated with 0.1, 0.25, 0.5 and 1.0 mg mL^{-1} PSS-FITC or PA-FITC respectively. A fixed incubation time of 30 min was used. The thickness and average fluorescence intensity of the fluorescent polymeric layer were determined from area measurements of confocal images using ImageJ software (Scion Corp., USA). Measurements were made from capsules ranging 30 to 60 µm in diameter, dispersed in the organic phase. The average fluorescence intensity measurements correspond to the density of the polymeric layer.

Demonstration of the Discrete Porosity Differences within Hydrogel Microspheres: Agarose microbeads were assembled with four layers of polymer $(PA/PSS)_2$ via the inwards interweaving self-assembly technique. A fixed polymer concentration of 0.5 mg mL^{-1} and incubation time of 30 min was used. The capsules were then transferred from 1-butanol to PBS buffer by first washing twice with ethanol containing 0.5% ADOGEN 464 and then with PBS/ethanol solutions of increasing PBS content (0.01×; 10%, 50%, and 90%) before transferring to pure 0.01× PBS. Microcapsules separately encapsulating 1 mg mL^{-1} of different molecular weight Dextrans (M_w 3000–5000 g mol^{-1}, 65 000–85 000 g mol^{-1} and 2 000 000 g mol^{-1}) were transferred into 0.01× PBS buffer and incubated for 24 h. The agarose microspheres were then observed under a confocal microscope.

Optical and Fluorescence Microscopy: Phase contrast and fluorescence microscopic images were recorded using a CCD color digital camera, Retiga 4000R (QImaging, Canada) connected to a system microscope (Olympus BX41) with a mercury arc (Olympus HBO103W/2) excitation source. Images were captured with QCapture Pro software (Version 5.1.1.14, QImaging, Canada) and analyzed by ImageJ software (Scion Corp., USA). Confocal fluorescence microscopic images were captured using a laser scanning confocal microscope, FluoView FV300 (Olympus Corp., Japan).

Supporting Information

Supporting Information is available from the Wiley Online Library or from the author.

Acknowledgements

This work was supported by Research grants R-397-000-077-112 and R182-000-200-112 from the National University of Singapore.

Received: February 27, 2013
Revised: April 8, 2013
Published online: May 27, 2013

[1] S. Jeon, V. Malyarchuk, J. O. White, J. A. Rogers, *Nano Lett.* **2005**, *5*, 1351.
[2] J. Q. Brown, R. Srivastava, M. J. McShane, *Biosens. Bioelectron.* **2005**, *21*, 212.
[3] P. Gupta, K. Vermani, S. Garg, *Drug Discovery Today* **2002**, *7*, 569.
[4] S. C. Chen, Y. C. Wu, F. L. Mi, Y. H. Lin, L. C. Yu, H. W. Sung, *J. Controlled Release* **2004**, *96*, 285.
[5] J. L. Drury, D. J. Mooney, *Biomaterials* **2003**, *24*, 4337.
[6] H. Tan, C. R. Chu, K. A. Payne, K. G. Marra, *Biomaterials* **2009**, *30*, 2499.
[7] A. D. Augst, H. J. Kong, D. J. Mooney, *Macromol. Biosci.* **2006**, *6*, 623.
[8] M. Lahaye, C. Rochas, *Hydrobiologia* **1991**, *221*, 137.
[9] W. C. Mak, K. Y. Cheung, D. Trau, *Chem. Mater.* **2008**, *20*, 5475.
[10] M. Delcea, A. Yashchenok, K. Videnova, O. Kreft, H. Möhwald, A. G. Skirtach, *Macromol. Biosci.* **2010**, *10*, 465.
[11] O. Kreft, M. Prevot, H. Möhwald, G. B. Sukhorukov, *Angew. Chem. Int. Ed.* **2007**, *46*, 5605.
[12] M. Delcea, N. Madaboosi, A. M. Yashchenok, P. Subedi, D. V. Volodkin, B. G. De Geest, H. Mohwald, A. G. Skirtach, *Chem. Commun.* **2011**, *47*, 2098.
[13] A. M. Yashchenok, M. Delcea, K. Videnova, E. A. Jares-Erijman, T. M. Jovin, M. Konrad, H. Möhwald, A. G. Skirtach, *Angew. Chem. Int. Ed.* **2010**, *49*, 8116.
[14] H. Bäumler, R. Georgieva, *Biomacromolecules* **2010**, *11*, 1480.
[15] J. Bai, S. Beyer, W. C. Mak, R. Rajagopalan, D. Trau, *Angew. Chem. Int. Ed.* **2010**, *49*, 5189.
[16] E. Poptoshev, B. Schoeler, F. Caruso, *Langmuir* **2004**, *20*, 829.
[17] N. S. Zacharia, M. Modestino, P. T. Hammond, *Macromolecules* **2007**, *40*, 9523.
[18] S. Beyer, J. Bai, A. M. Blocki, C. Kantak, Q. Xue, M. Raghunath, D. Trau, *Soft Matter* **2012**, *8*, 2760.
[19] S. Arnott, A. Fulmer, W. E. Scott, I. C. M. Dea, R. Moorhouse, D. A. Rees, *J. Mol. Biol.* **1974**, *90*, 269.

© 2013 WILEY-VCH Verlag GmbH & Co. KGaA, Weinheim

[20] J. Bai, S. Beyer, S. Y. Toh, D. Trau, *ACS Appl. Mater. Interfaces* **2011**, *3*, 1665.
[21] M. Duckworth, W. Yaphe, *Carbohyd. Res.* **1971**, *16*, 189.
[22] J. Minghou, M. Lahaye, W. Yaphe, *Chin. J. Ocean. Limnol.* **1988**, *6*, 87.
[23] I. Braccini, S. Pérez, *Biomacromolecules* **2001**, *2*, 1089.
[24] A. Martinsen, G. Skjak-Braek, O. Smidsrod, *Biotechnol. Bioeng.* **1989**, *33*, 79.
[25] R. Zhang, K. Kohler, O. Kreft, A. Skirtach, H. Mohwald, G. Sukhorukov, *Soft Matter* **2010**, *6*, 4742.
[26] S. Beyer, W. C. Mak, D. Trau, *Langmuir* **2007**, *23*, 8827.
[27] A. A. Antipov, G. B. Sukhoruko, S. Leporatti, I. L. Radtchenko, E. Donath, H. Möhwald, *Colloids Surf. A* **2002**, *535*, 198.
[28] D. V. Volodkin, A. I. Petrov, M. Prevot, G. B. Sukhorukov, *Langmuir* **2004**, *20*, 3398.

© 2013 WILEY-VCH Verlag GmbH & Co. KGaA, Weinheim